Journal of Molecular Graphics and Modelling 54 (2014) 1–9

Contents lists available at ScienceDirect

Journal of Molecular Graphics and Modelling

journal homepage: www.elsevier.com/locate/JMGM

Molecular recognition pattern of cytotoxic alkaloid vinblastine with multiple targets

Prateek Pandya[a], Lokesh Kr Agarwal[a], Neelima Gupta[a,*], Sourav Pal[b]

[a] Department of Chemistry, University of Rajasthan, Jaipur, India
[b] Physical Chemistry Division, CSIR-National Chemical Laboratory, Pune, India

ARTICLE INFO

Article history:
Accepted 2 September 2014
Available online 16 September 2014

Keywords:
Drug–DNA interactions
Drug–protein binding
Vinblastine
Multitarget affinity
Human serum albumin
Molecular docking
QM–MM calculation

ABSTRACT

Vinblastine (VLB), a cytotoxic alkaloid is used extensively against various cancer types and the crystal structure of its tubulin complex is already known. Multitarget affinity of vinblastine has been investigated and the nature of binding with biological receptors namely, duplex DNA and Human serum albumin (HSA) has been compared to the binding characteristics of its known complex with natural high affinity receptor tubulin using molecular docking and QM–MM calculations. VLB is found to interact with DNA as well as HSA protein, though, with weaker affinity as compared to tubulin. Analysis of various docked complexes revealed that the H-bonds and cation–pi bonds do not have significant contribution to the binding interactions and despite its large size, VLB remains in relaxed conformation and fits in the hydrophobic regions on the receptors.

1. Introduction

Vinblastine (VLB; Fig. 1) is a well-known anticancer agent effective against several types, such as Hodgkin's disease, lymphocytic lymphoma, histiocytic lymphoma, advance testicular cancer, advanced breast cancer, Kaposi's sarcoma and Letterer–Siwe disease [1–3]. Studies pertaining to VLB's physiological and therapeutic effects were initiated around the same time as that of the discovery of DNA double helix [4]. VLB is known to interact with a variety of biological macromolecules like proteins and nucleic acids [5–10]. The X-ray crystal structures of vinblastine sulfate [11] as well as VLB–tubulin complex [10] have already been reported. The interaction of VLB with human serum albumin (HSA) was investigated long ago on the leukemia cell line MOLT-3 using cell based assay technique [12], which had indicated for the first time that VLB binds weakly with human serum albumin protein. In addition, VLB's ability to interact with different types of molecules has also been identified in nanoparticle mediated drug delivery efforts. Effective delivery of VLB has been explored using various nanoparticles such as poly(lactide-co-glycolide) [13], liposomes [14], etc. Since albumin is a highly suitable material for use as nanoparticles for drug delivery mechanisms [15], a number of studies have been accomplished on the preparation of vinblastine loaded nanoparticles of serum albumin protein [16].

The information regarding the nature of binding with biomolecules, especially with proteins, nucleic acids, etc. is essential in order to understand the mechanism of their interactions and to identify similar possible ligands of potential medicinal importance. A survey of literature reveals that the exact nature of binding of vinblastine with multiple receptor targets and the detailed structural aspects of VLB-HSA interactions in particular has not been investigated thoroughly. Molecular docking is a fast and reliable tool for the study of inter-molecular interactions in the systems of biological and therapeutic significance. Although, the QM–MM approach, that combines the accuracy of quantum mechanics and speed of molecular mechanics, was introduced as early as 1970s by Warshel and Levitt [17] to obtain more realistic information about biomolecular interactions, most of the early stages of drug discovery process still involve the use of the molecular mechanics based docking programs to obtain dependable prediction toward the efficacy of the pharmaceutically important molecules [18–22]. Several docking programs with varied capabilities are available for calculating interactions with different biomolecules, some of them having their own limitations to explore specific regions on receptor molecule, e.g. major/minor grooves of DNA. Recently, a comparison between various computational docking methods suitable for studying minor groove DNA binders has been made [23]. The effect of the conformational preferences in several natural and

* Corresponding author. Tel.: +91 1412722340.
E-mail addresses: prateekpandya@gmail.com (P. Pandya), lokeshmittal24@gmail.com (L.K. Agarwal), guptaniilima@gmail.com (N. Gupta), s.pal@ncl.res.in (S. Pal).

http://dx.doi.org/10.1016/j.jmgm.2014.09.001
1093-3263/

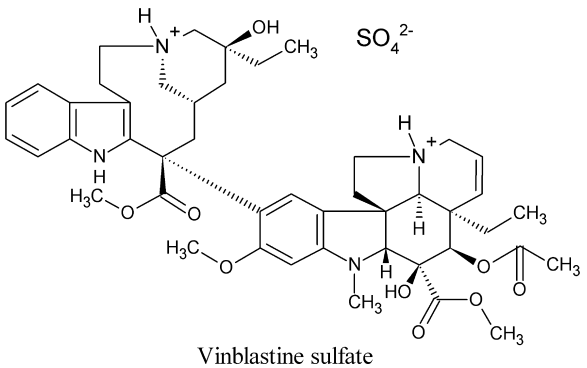

Fig. 1. Structure of vinblastine sulfate.

semi-synthetic vinca alkaloid molecules on their affinity to tubulin has been investigated previously by Kelly et al. [24] at semiempirical AM1 level using QM-MD simulations. In the present investigation, an attempt has been made to identify the nature of binding interactions of vinblastine with biological receptors such as duplex DNA and Human serum albumin using molecular docking program AutoDock-vina and applying QM–MM based ONIOM methodology. The binding characteristics of VLB–DNA/VLB–HSA complexes and their dependence on stable conformation have been compared with that of natural high affinity receptor tubulin.

2. Materials and methods

Molecular docking calculations were carried out using AutoDock-vina program from The Scripps Research Institute [25]. Rigid body docking program DNADock [26], used in an earlier study of VLB–DNA binding [5], had limitation to explore only the DNA minor groove binding space without any structural perturbations in DNA. The resulting docked structures were highly strained and no significant binding forces could be identified in the minor groove poses. AutoDock-vina program was used in present study because it has the option to explore both the minor and major groove binding modes and is reported to perform faster and do more accurate calculations than Autodock software [27–32].

CD experiments were conducted on a Jasco J-815 spectropolarimeter in the spectral region 210–400 nm to monitor the drug induced conformational changes of the DNA structure [30]. VLB is an optically active drug having active CD pattern in the same region of DNA peaks, making difficult assessment of structural changes on complexation. Hence, two separate titrations between VLB-DNA and VLB-Buffer were performed. Circular dichroism (CD) experiments performed with VLB and DNA indicated that no significant perturbation occurs in DNA structure, therefore, the flexibility option for the receptor biomolecule was not included.

For molecular docking calculations, the receptor and drug coordinate files were converted into PDBQT format using MGLTools (version 1.5.4). 3D structure of vinblastine dication was prepared in PDB format from its X-ray geometry [11] using Discovery Studio Visualizer 3.0. Four B-form DNA sequences (Table 1), as used in the previous study [5], were utilized to study the possibility of sequence specific interaction with any of the chosen four complementary central base pair combinations.

Table 1
Four B-DNA decamer sequences used for docking calculations.

	DNA sequence
S1	5′-d(GATGGCCATC)$_2$
S2	5′-d(GATCCGGATC)$_2$
S3	5′-d(GGCAATTGCC)$_2$
S4	5′-d(GGCTTAAGCC)$_2$

Docking of VLB with four DNA sequences was performed using vina program with a large grid box (size $28 \times 26 \times 36$ with grid center at $x = -0.668$, $y = 0.358$, $z = 15.0$) so as to accommodate both the major and the minor grooves of DNA. DNA docking was carried out with increased exhaustiveness of 32 which is four times the default value in Autodock-vina program. This helped in evaluating the preference of VLB toward one or the other grooves. HSA structure file was obtained from Protein Data Bank (PDB) [HSA PDB ID 1E7A] and for docking calculations, a three-dimensional grid box of size $44 \times 48 \times 40$ centered on coordinates $x = -1.101$, $y = -10.483$, $z = -0.224$ was prepared with a grid spacing of 1.0 Å. Due to the larger size of the grid box, in this case also the calculations were performed at the exhaustiveness of 32 in Autodock-vina program. For each docking calculation, 20 different poses were requested within the energy range of 2 kcal mol^{-1} to sample greater variation in poses. All other parameters were kept at their default values. The choice of docking with a single program (vina) enabled effective comparison of VLB's binding with different receptors.

2.1. Docking standardization procedure

In order to obtain reliable docking results, standardization was done by reproducing the crystal structure of the vinblastine–tubulin complex using Autodock-vina program as described [32]. Vinblastine–tubulin complexes (PDB ID 1Z2B and 4EB6) were studied for their binding motifs. The PDB file of Vinblastine–tubulin complex was taken from the PDB (ID 1Z2B) and VLB molecule was removed from the complex. Vinblastine was then allowed to dock onto the tubulin protein at the original binding site to obtain binding poses with minimum deviation from the crystal structure. Interestingly, the docking calculation produced only one pose in the defined pocket, which was laid over the original crystal structure pose by superimposing the indole rings to assess any deviations in conformation. The binding pose of VLB was found to be almost same as in the original VLB–Tubulin complex crystal structure (Fig. 2a and Table 2) validating the choice of docking program. The analysis of docking results was carried out using Discovery Studio Visualizer, UCSF-Chimera (version 1.8) and MOE software.

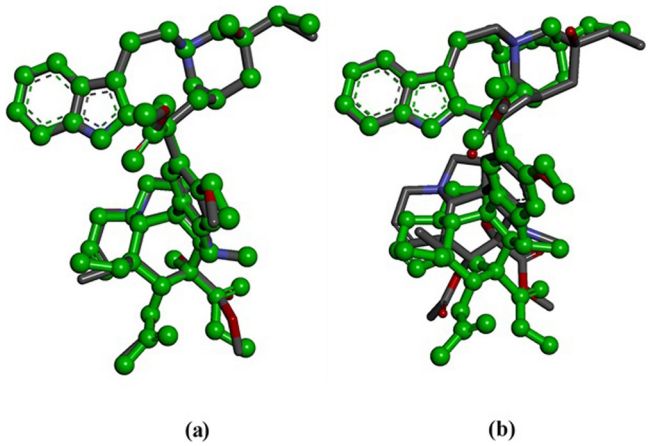

Fig. 2. Superimposition of crystal geometry (green ball and stick model) of VLB in VLB–tubulin complex extracted from PDB 1Z2B – (a) with vina-docked pose (stick model) of VLB in VLB–tubulin complex; and (b) with crystal structure of isolated VLB molecule (stick model) [11]. (For interpretation of the references to color in this figure legend, the reader is referred to the web version of the article.)

Table 2
Selected distances (Å) and dihedral angle showing distortion in VLB geometry after interaction with tubulin and DNA. VLB molecule sketch showing atom numbering used

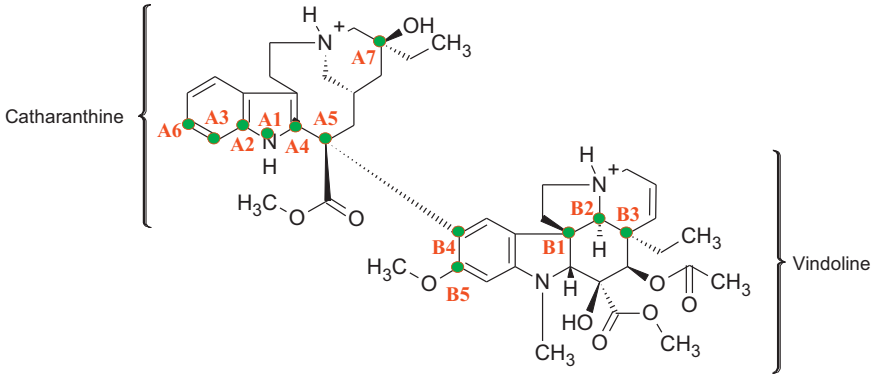

to calculate distances

	VLB	VLB–tubulin		VLB–DNA							
	Crystal[a]	Crystal[b]	Docked[c]	Major groove				Minor groove			
				S1	S2	S3	S4	S1	S2	S3	S4
A1–B1[d]	5.24	5.15	5.20	4.95	4.94	4.98	5.01	7.36	7.51	7.51	6.41
A2–B2	5.60	5.41	5.45	5.20	5.20	5.19	5.20	9.22	9.18	9.24	8.97
A3–B3	6.53	6.32	6.33	6.11	6.13	6.07	6.05	12.07	12.05	12.18	11.88
A6–A7	9.50	8.98	8.98	9.59	9.59	9.59	9.59	9.18	8.59	8.61	8.73
ω1[e]	−162.1	−146.6	−143.8	−171.8	−173.1	−169.1	−166.7	−36.4	−41.1	−45.0	−23.0

[a] CCDC Number: 207/438 Ref. [11].
[b] PDB ID 1Z2B.
[c] Docked pose of VLB onto tubulin molecule in present study.
[d] A – atom from catharanthine half; B – atom from vindoline half, numbering as per above structure.
[e] ω1 = torsion angle A4–A5–B4–B5.

2.2. ONIOM QM–MM calculation procedure

Two layer ONIOM calculation [33] was carried out using Gaussian-09 [34]. The calculation was performed using best binding docked pose of VLB with DNA sequence S1. For this purpose, the VLB molecule was treated in high (QM) layer while the DNA was treated with MM. The idea was to further optimize the VLB pose resulting from docking using Quantum mechanics while keeping VLB within the influence of DNA major groove. The calculation was done for QM layer at DFT level with B3LYP/6-31G* basis set and treating the DNA in MM layer using amber force field.

3. Results and discussion

The interaction pattern of large size drugs with biomolecules is strongly influenced by the adoption of a particular conformation and vise-versa. The structure of VLB (Fig. 1) possesses significantly hydrophobic regions incorporating indole and indoline moieties apart from the presence of certain electronegative groups that are capable of forming H-bonds. At the same time, about half of the VLB population is known to exist as positively charged form at neutral pH in solution. Stable conformation of the drug molecule in a biological system is a result of a balance of various binding forces and an insight to various conformations is best obtained from a quantum mechanical (QM) methodology. In a number of recent studies, the density functional theory (DFT)-based methodologies have been successfully applied for this purpose [35,36]. In the present case, the geometry of the VLB dication optimized at the DFT (B3LYP/6-31G*) level is found quite similar to the reported crystal structure of vinblastine sulfate. Therefore, in order to understand the interaction pattern of VLB with multiple biological receptors – tubulin, DNA and HSA, the docking calculations were performed by taking the dipositive form of VLB. The results from various sets of calculations are described below.

3.1. Vinblastine–tubulin complex

VLB is an unusually large sized molecule to be called as drug in the conventional sense (as described by Lipinski et al. [37,38]). However, VLB's utility in cancer chemotherapy is undisputed as it is one of the most commonly used drug of natural origin. Vinblastine is known to have higher affinity with β-tubulin causing microtubule disassembly [39]. The crystal structure of VLB–tubulin complex [10] illustrates the presence of VLB molecule at the interface of α and β subunits (Fig. 3a). Significant binding of VLB with β subunit at inter–dimer interface have been shown to introduce curvature in tubulin assemblies causing microtubule depolymerization.

Visualization of the VLB–tubulin complex in the form of an interaction diagram (Fig. 3b) clearly shows that VLB comfortably rests in the binding pocket on tubulin without much strain. The binding is largely stabilized by hydrophobic forces along with the presence of two H-bonds between oxygen atoms of VLB and the amino acids Asparagine and Proline of tubulin. The binding affinity of the docked VLB–tubulin complex structure is -10 kcal mol^{-1}, which is quite high for a drug–protein complex. It is most likely due to the fact that the VLB is highly hydrophobic and the volume of the binding pocket is sufficient to accommodate the lipophilic VLB molecule in relaxed conformation. In addition, the VLB molecule in the bound state is less solvent exposed (Fig. 3b) making it a good candidate for stronger affinity toward tubulin. Thus it is apparent that the overall binding of VLB with tubulin is driven by the hydrophobic contacts that it makes with the protein residues. It may be noted that the conformation of VLB has not changed significantly in its tubulin complex when compared to crystal geometry of isolated VLB molecule (Fig. 2b). Notable conformational changes in the tubulin-bound form include some twisting of the torsion angle between indole and indoline rings and slight decrease in the flatness of the catharanthine half as evident from 0.5 Å decrease in A6–A7 distance (Table 2). With this information, we have now analyzed the binding

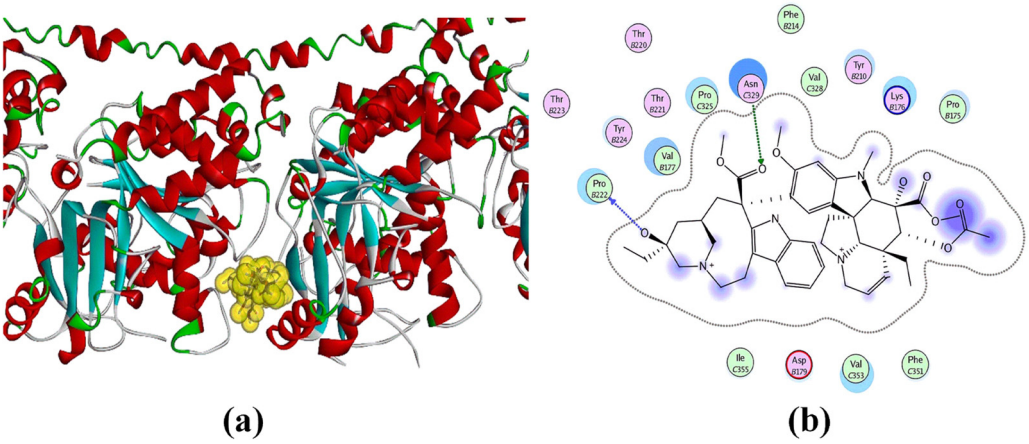

Fig. 3. (a) Crystal structure of VLB–tubulin complex (PDB ID 1Z2B) with vinblastine in the middle shown with van der Waals surface, (b) two H-bonds visible in interaction diagram of VLB–tubulin complex (blue shaded area showing solvent exposed parts of VLB molecule). (For interpretation of the references to color in this figure legend, the reader is referred to the web version of the article.)

of VLB with other receptors viz., DNA and Human Serum Albumin (HSA) protein to decipher its molecular recognition pattern.

3.2. Vinblastine–DNA binding

Vinblastine has been reported to bind with double stranded DNA at two different sites viz., major and minor grooves of DNA on the basis of several experimental reports [5–7]. Therefore, in the present study, extensive docking calculations have been performed with Autodock-vina program with the possibility to explore both major and minor grooves of DNA and obtain a clearer picture about the preference of VLB toward either of the DNA grooves. However, it is interesting to note that in case of all four selected B-DNA sequences, the resulting docked poses of VLB lie only in the major groove (Fig. S1, Supplementary information), showing no sequence specificity.

Most minor groove binding ligands have curved shape structures which facilitate them to fit into the narrow minor groove of B-DNA duplex [40]. Therefore, if a large molecule like VLB interacts with minor groove of DNA, then either a significant perturbation of DNA structure is required to accommodate it or the conformation of the drug molecule has to be modified so as to fit into the minor groove. In the latter case, the drug molecule would be under significant strain from its most stable conformation. In the present study, though, the grid-box of enough large size provided flexibility to the VLB for binding with both DNA grooves; no docked pose was obtained in the minor groove. The relative strain in the major groove docked poses obtained from the present study has been compared with the DNA minor groove docked poses obtained from previous investigation [5] using DNADock by superimposing the docked geometries onto the crystal structure of isolated VLB molecule (Fig. 4a and b).

Selected distances and the torsion angle ω1 (A4-A5-B4-B5) listed in Table 2 reveal that conformation of the major groove pose (Fig. 5a) is almost as much relaxed as in the VLB crystal (Fig. 5b) without any significant deformation in the flatness of catharanthine half. It may be inferred that the puckered shaped conformation of VLB does not allow it to fit easily into the minor groove of DNA and for making any minor groove binding possible, the vindoline half has to flip out taking the indole and indoline rings away from each other (Figs. 4b and 5c). When compared to the isolated crystal, tubulin complex and DNA major groove conformations

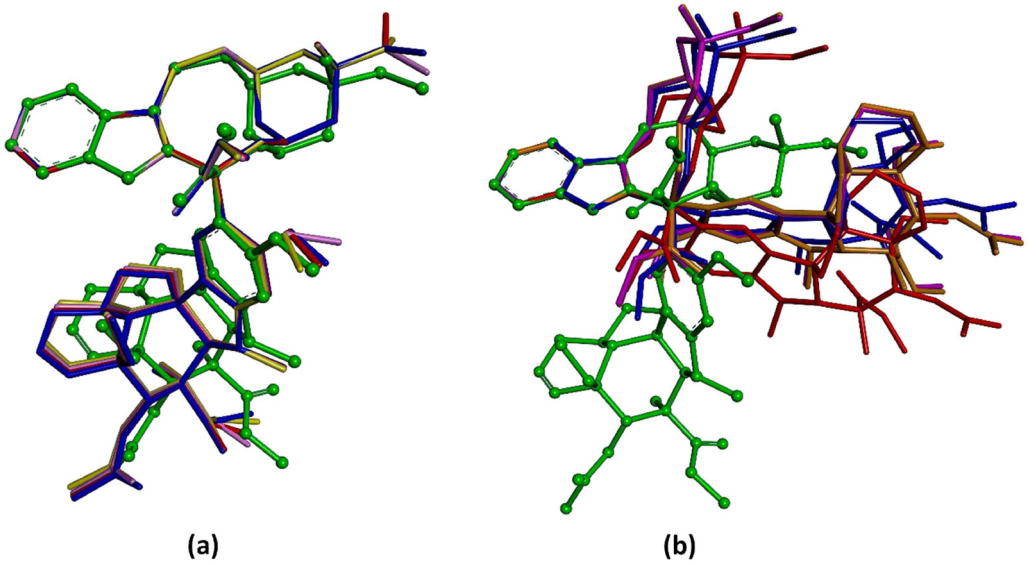

Fig. 4. Overlay of VLB crystal structure [11] (green ball and stick model) with best binding poses (stick model) (a) from major groove docked DNA–VLB complex obtained from Autodock-vina (b) minor groove binding poses obtained from DNADock [5].

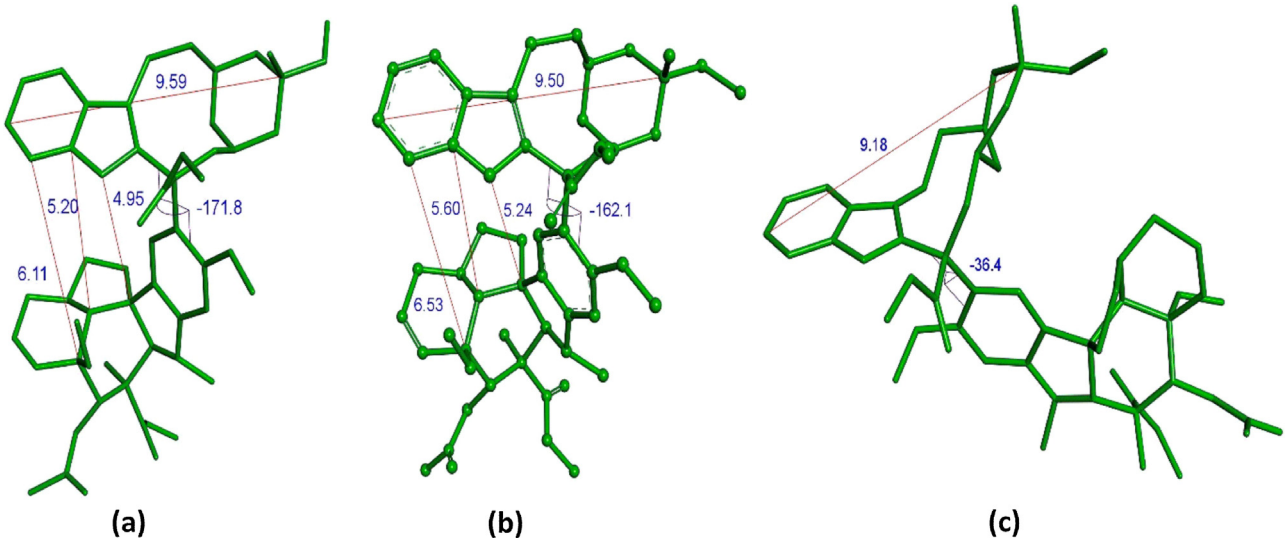

Fig. 5. conformations of VLB in (a) major groove pose, (b) VLB crystal structure, (c) minor groove binding pose.

(Table 2), the twisting in minor grove pose (Fig. 5c) is substantial ($\omega 1 = 36.4^{\circ}$) and is accompanied with the folding of catharanthine part (A6–A7 = 9.1 Å), thereby creating much steric constraints in minor groove poses.

Thus, in contrast to many other conventional drugs that are known to bind in the minor groove of DNA [41], the preference for major groove binding of VLB may be attributed to slightly twisted orientation of two halves that makes it fit easily in the space available without any additional constraints. In a recent experimental study based on IR data [6] also, the VLB molecule has been suggested to preferably interact with the major groove of DNA. Analysis of the interaction diagrams of major groove binding poses obtained from present docking calculations shows that VLB–DNA binding is stabilized largely via van-der-Waals forces along with other stabilizing interactions such as H-bonds (Fig. 6) and in some cases cation–pi bonds.

Graphical presentation of the binding free energy and the distribution of H-bonds/cation–pi bonds in the docked poses has been shown in Fig. 7 (detailed bar diagram – Fig. S2 available in supplementary information). It may be noted that only few poses possess both the H-bond and cation–pi interactions and in majority of binding poses either of the two is present. Out of the total 80 docked structures obtained from all the four DNA sequences, almost equal number of H-bonds (31) and cation–pi bonds (29) were observed. However, the maximum number of H-bonds was detected in VLB–S3 complexes while maximum cation–pi bonds

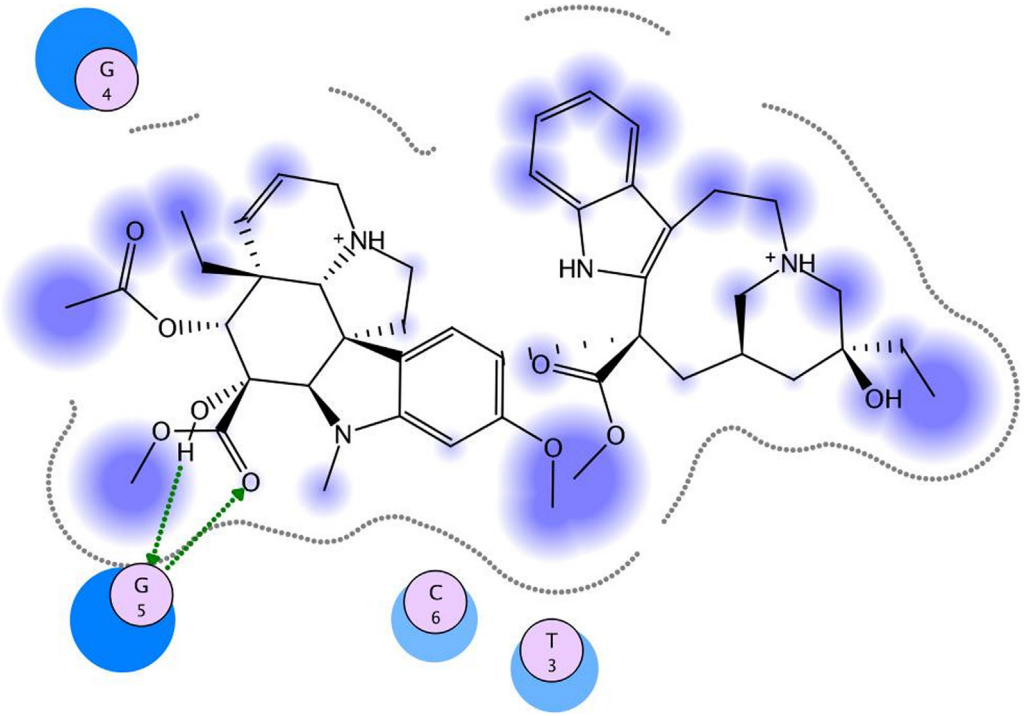

Fig. 6. VLB–DNA Interaction diagram showing bifurcated H-bonding between G5 of DNA and vinblastine molecule.

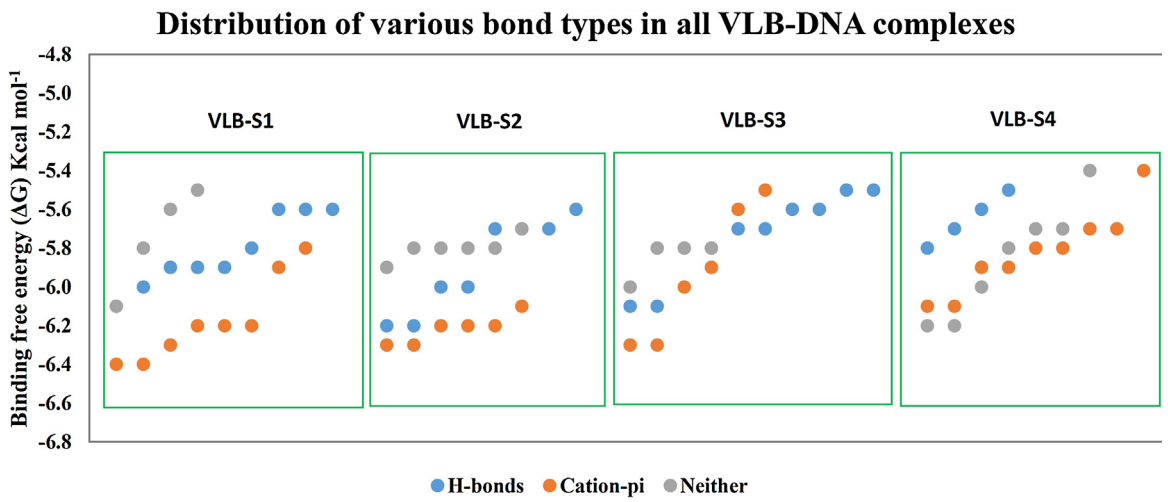

Fig. 7. Distribution of VLB–DNA docked poses according to the type of bonds present.

were observed in VLB–S4 complexes. Though, the presence of H-bonds or cation–pi bonds has not been found to affect the binding affinity significantly. The analysis does not reveal any specific pattern correlating binding affinity with H-bonds or cation–pi bonds. Besides, It is not necessary that the maximum binding affinity pose has H-bond or cation–pi bond interaction. Interestingly, all the docked structures showed similar range of binding affinity values (from −6.5 to −5.4 kcal mol^{-1}), irrespective of the DNA sequence design indicating that VLB–DNA interaction is not sequence specific and mainly stabilizes with van-der-Waals forces. These results show that if a proper space is explored around both the grooves of DNA, the preference of VLB is always greater for the major groove as compared to the minor groove.

QM–MM ONIOM Calculation: The conformation of the best binding VLB poses (Fig. 4) obtained from docking calculation are a result of the treatment of both the VLB and DNA by molecular mechanics. In order to treat the VLB with more precise QM method while treating the DNA with MM method, ONIOM calculation was performed on VLB–S1(DNA) complex using two layer method where the DNA was considered as rigid molecule and the VLB in the bound state was subjected to geometry optimization at DFT level. The ONIOM calculation was successful for VLB–DNA major groove complex but could not be completed for DNA minor groove complex even after repeated attempts. The two layer ONIOM (B3LYP/6-31G*:Amber) calculation was done considering the VLB–DNA complex as real system and VLB molecule as model system for low(MM) and high(DFT) level calculations, respectively. The extrapolated energy E_1 (−2683.7320566 a.u.) for VLB–S1(DNA) system during ONIOM calculation has been obtained as per Eq. (1).

$$E_1(\mathrm{VLB-S1})_{\mathrm{ONIOM}} = E_2(\mathrm{VLB-S1})_{\mathrm{MM}} + E_3(\mathrm{VLB})_{\mathrm{QM}} - E_4(\mathrm{VLB})_{\mathrm{MM}} \quad (1)$$

where $E_2(\mathrm{VLB-S1})_{\mathrm{MM}}$ is the energy of real system (VLB–S1 complex) obtained from amber force field treatment and the $E_3(\mathrm{VLB})_{\mathrm{QM}}$ and $E_4(\mathrm{VLB})_{\mathrm{MM}}$ are the energy of Model system (VLB in bound form) obtained from DFT and amber treatment, respectively. The interaction energy E_5 of the VLB–S1 complex can be obtained from the Eq. (2)

$$E_5 = E_1(\mathrm{VLB-S1})_{\mathrm{ONIOM}} - (E_6(\mathrm{VLB})_{\mathrm{QM}} + E_7(\mathrm{S1})_{\mathrm{MM}}) \quad (2)$$

where $E_6(\mathrm{VLB})_{\mathrm{QM}}$ is the QM energy of isolated VLB and $E_7(\mathrm{S1})_{\mathrm{MM}}$ the Amber energy of DNA alone. As during the ONIOM calculation the DNA layer was kept rigid without optimization

$$E_7(\mathrm{S1})_{\mathrm{MM}} \approx E_2(\mathrm{VLB-S1})_{\mathrm{MM}} - E_4(\mathrm{VLB})_{\mathrm{MM}} \quad (3)$$

On putting the values of E_1 from Eq. (1) and E_7 from Eq. (3) into Eq. (2), the interaction energy E_5 becomes equal to $E_3(\mathrm{VLB})_{\mathrm{QM}}$–$E_6(\mathrm{VLB})_{\mathrm{QM}}$. On using the values of E_2 (0.9813832 a.u.), E_3 (−2684.5446716 a.u.) and E_4 (0.1687682 a.u.) as obtained from ONIOM and E_6 (−2684.5540414 a.u.) from QM calculation of isolated VLB, the interaction energy E_5 of VLB-DNA major groove

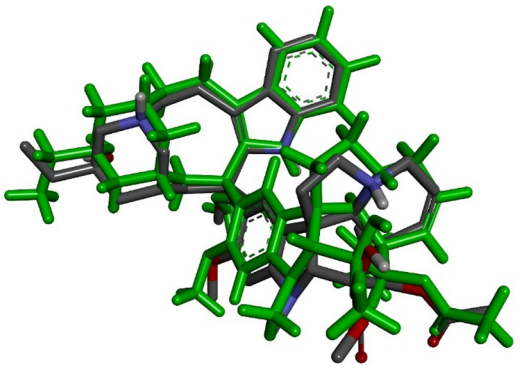

Fig. 8. Overlay of ONIOM optimized structure of VLB (green color) with docked structure of VLB in VLB–DNA complex.

Table 3
Binding free energy (in kcal mol^{-1}) of VLB with various receptors.

	DNA sequences				HSA	Tubulin
	S1	S2	S3	S4		
ΔG max	−6.40	−6.30	−6.30	−6.20	−7.6	−10
ΔG min	−5.50	−5.60	−5.50	−5.40	−6.4	–
Solvent exposed regions	Highest	Higher	Lowest			

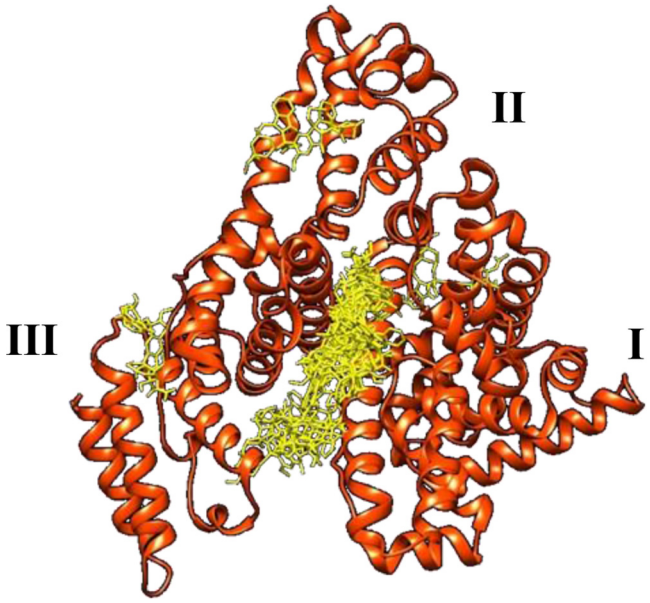

Fig. 9. VLB–HSA complex. VLB docked poses (yellow) are seen at various binding sites on HSA. (For interpretation of the references to color in this figure legend, the reader is referred to the web version of the article.)

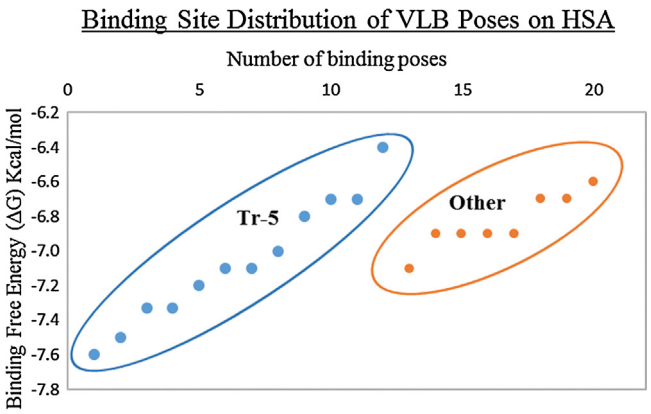

Fig. 10. Distribution of VLB poses on the HSA molecule with majority of poses in the Tr-5 region of HSA (Details in Table S4 of supplementary information).

complex came out to be −5.88 kcal mol^{-1} which is quite close to the values obtained from VLB–DNA docking calculations (Table 3).

In addition, an overlay of the QM optimized VLB geometry from ONIOM calculation on the docked geometry (Fig. 8) reveals that there is not much deviation in the two conformations of VLB–DNA major groove complex. Thus the QM–MM method also supports the binding preference of VLB in the DNA major groove.

3.3. Vinblastine–HSA binding

The structure of Human serum albumin (HSA), which consists mainly of α-helices and no β-sheets, contains three homologous domains, viz., Domain I, II and III (Fig. 9). Thus, HSA is a multi-domain carrier molecule which binds to a large array of molecules with its various domains [42–46]. The wide-ranging variety of HSA binding molecules includes drugs, fatty acids, hormones and even proteins and peptides [47]. Several binding sites exist on HSA molecule for variety of ligand molecules [48]. To have an idea about the most probable binding site on HSA for VLB molecule, a blind rigid body docking was performed covering the entire HSA molecule. This resulted in several docked poses at various binding sites as shown in Fig. 9.

It is evident from the docking analysis that VLB prefers to sit in the middle Tr-5 region of HSA molecule (Fig. 9). The Tr-5 consists of a wide-spaced region flanked by the helices of domain I, II and subdomain IIIA and is also one of the sites for Thyroxine molecule [48]. In the present case also, maximum number of VLB poses (12 poses out of 20) are found to be in this region as evident from Fig. 10.

As clearly seen in the three dimensional interaction surface (Fig. 11A), the larger part of VLB molecule is associated with hydrophobic interactions (green surface). Further, the interaction diagram (Fig. 11B) confirms that the Tr-5 region provides sufficient surface area for the stability of VLB–HSA complex.

The interaction diagram of VLB with HSA residues (Fig. 11B) reveals that Tr-5 is the best suited site for bigger molecules like VLB because of the availability of relatively large space and less solvent exposed area as compared to DNA. It is interesting to note that the binding free energy values obtained from VLB-HSA docking are higher (in the range of −7.6 to −6.4 kcal mol^{-1}, Table 3) than those with any of the four DNA sequences (S1–S4). However, when compared with VLB–tubulin complex, the Tr-5 site in HSA is more solvent exposed and therefore, provides less binding affinity for VLB complexation.

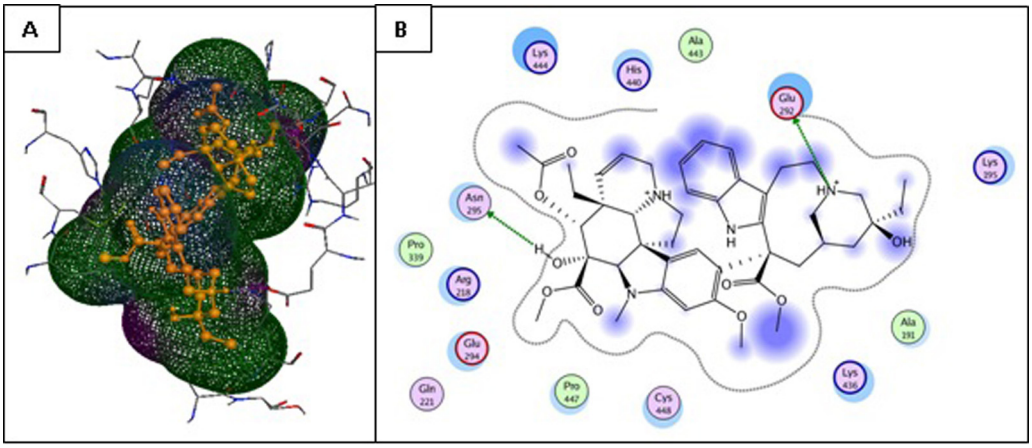

Fig. 11. (A) VLB in the Tr-5 binding pocket. Green colored surface indicates hydrophobic contacts. (B) Interaction map of VLB pose with HSA molecule. Blue shading in (B) indicates solvent exposed regions. (For interpretation of the references to color in this figure legend, the reader is referred to the web version of the article.)

4. Conclusion

In the present study, the interaction profile of VLB with duplex DNA and HSA protein has been analyzed viz. a viz. VLB–tubulin complex in order to obtain an understandable picture about the molecular recognition signature of VLB using molecular docking and QM–MM calculations. A comparison of our docking results with the previously reported crystal structure of VLB–tubulin complex, validates the efficiency of the adopted docking methodology which has been further applied to obtain important insight into the behavior of VLB toward other receptors such as DNA and HSA. The number of H-bonds or cation–pi bonds in these complexes has not revealed any significant pattern to explain binding affinity variations. It may be inferred that a large sized molecule like VLB, tends to approach a particular site of biomolecule which provides sufficient space for the former to remain in a relatively relaxed conformation, as indicated by the similarity of bound poses to the crystal geometry of the isolated VLB. QM–MM calculation in one case further supports that large molecules like VLB tend to drive toward the receptor via van der Waals forces which enable it to hold on to the receptor site with multiple contacts. It is therefore concluded that the actual hydrophobic regions of a large molecule may contribute more toward binding as compared to the associated H-bond donor/acceptor atoms. Although, it is known that the presence of specific H-bonds impart binding specificity in DNA minor groove ligands, the H-bonding pattern becomes less significant when the binding is weak and non-specific. The trend of binding free energy values of VLB–tubulin, VLB–HSA and VLB–DNA complexes, further suggest that the increasing solvent exposure of VLB, directly affects the hydrophobic contacts between bound pose of VLB and the receptor molecules and consequently reduces the overall binding affinity.

Supplementary information

Binding free energy (ΔG in kcal mol^{-1}) and number of Hydrogen and cation–pi bonds in docked poses of VLB–DNA sequences S1–S4. Binding site landscape of VLB–HSA interactions at Tr-5 and other binding sites. Graphical presentation of VLB–DNA interactions. Optimized coordinates from two layer ONIOM (B3LYP/6-31G*:Amber) calculation.

Acknowledgements

P. P. acknowledges the UGC, New Delhi for the award of Dr. D.S. Kothari PDF No. F.4-2/2006(BSR)/13-557/2011. Financial assistance from the DST, New Delhi (Grant no. SR/S1/OC-21/2008) is duly acknowledged. We also thank Prof. Ritu Barthwal, Department of Biotechnology, IIT-Roorkee, India for providing us with their MOE program facility for the analysis of docked complexes.

Appendix A. Supplementary data

Supplementary data associated with this article can be found, in the online version, at http://dx.doi.org/10.1016/j.jmgm.2014.09.001.

References

[1] P.G. Gobbi, C. Broglia, F. Merli, M. Dell'Olio, C. Stelitano, E. Iannitto, M. Federico, R. Berte, D. Luisi, S. Molica, C. Cavalli, L. Dezza, E. Ascari, Vinblastine, bleomycin, and methotrexate chemotherapy plus irradiation for patients with early-stage, favorable Hodgkin lymphoma: the experience of the Gruppo Italiano Studio Linfomi, Cancer 98 (2003) 2393–2401.
[2] M.A. Jordan, L. Wilson, Microtubules as a target for anticancer drugs, Nat. Rev. Cancer 4 (2004) 253–265.
[3] B. Boll, H. Bredenfeld, H. Gorgen, T. Halbsguth, H.T. Eich, M. Soekler, J. Markova, U. Keller, U. Graeven, S. Kremers, M. Geissler, G. Trenn, M. Fuchs, B. von Tresckow, D.A. Eichenauer, P. Borchmann, A. Engert, Phase 2 study of PVAG (prednisone, vinblastine, doxorubicin, gemcitabine) in elderly patients with early unfavorable or advanced stage Hodgkin lymphoma, Blood 118 (2011) 6292–6298.
[4] J.R. Wright Jr., Almost famous: E. Clark Noble, the common thread in the discovery of insulin and vinblastine, Can. Med. Assoc. J. 167 (2002) 1391–1396.
[5] P. Pandya, S.P. Gupta, K. Pandav, R. Barthwal, B. Jayaram, S. Kumar, DNA binding studies of Vinca Alkaloids: experimental and computational evidence, Nat. Prod. Commun. 7 (2012) 305–309.
[6] G. Tyagi, S. Charak, R. Mehrotra, Binding of an indole alkaloid, vinblastine to double stranded DNA: a spectroscopic insight in to nature and strength of interaction, J. Photochem Photobiol. B 108 (2012) 48–52.
[7] J.M. Pezzuto, C.-T. Che, D.D. McPherson, J.-P. Zhu, G. Topcu, C.A.J. Erdelmeier, G.A. Cordell, DNA as an affinity probe useful in the detection and isolation of biologically active natural products, J. Nat. Prod. 54 (1991) 1522–1530.
[8] M. Semmel, Interaction in vitro between nucleic acids and the alkaloids extracted from *Vinca rosea* and glutamic acid, Biochimie 53 (1971) 457–460.
[9] S.P. Gupta, K. Pandav, P. Pandya, G.S. Kumar, R. Barthwal, S. Kumar, Methylene linker assisted DNA binding of vinblastine and simpler analogs: purine-pyrimidine specificity of indole derivatives, Chem. Biol. Interface 1 (2011) 297–309.
[10] B. Gigant, C. Wang, R.B.G. Ravelli, F. Roussi, M.O. Steinmetz, P.A. Curmi, A. Sobel, M. Knossow, Structural basis for the regulation of tubulin by vinblastine, Nature 435 (2005) 519–522.
[11] R. Bau, K.K. Jin, Crystal structure of vinblastine, J. Chem. Soc. Perkin Trans. 1 (2000) 2079–2082.
[12] I. Takahashi, T. Ohnuma, S. Kavy, S. Bhardwaj, J.F. Holland, Interaction of Human Serum Albumin with anticancer agents in vitro, Br. J. Cancer 41 (1980) 602–608.
[13] J. Marinina, A. Shenderova, S.R. Mallery, S.P. Schwendeman, Stabilization of vinca alkaloids encapsulated in poly(lactide-co-glycolide) microspheres, Pharm. Res. 17 (2000) 677–683.
[14] I.V. Zhigaltsev, N. Maurer, Q.F. Akhong, R. Leone, E. Leng, J. Wang, S.C. Semple, P.R. Cullis, Liposome-encapsulated vincristine, vinblastine and vinorelbine: a comparative study of drug loading and retention, J. Control. Release 104 (2005) 103–111.
[15] F. Kratz, Albumin as a drug carrier: design of prodrugs, drug conjugates and nanoparticles, J. Control. Release 132 (2008) 171–183.
[16] Y. Zu, Y. Zhang, X. Zhao, Q. Zhang, Y. Liu, R. Jiang, Optimization of the preparation process of vinblastine sulfate (VBLS)-loaded folate-conjugated bovine serum albumin (BSA) nanoparticles for tumor-targeted drug delivery using response surface methodology (RSM), Int. J. Nanomed. 4 (2009) 321–333.
[17] A. Warshel, M. Levitt, Theoretical studies of enzymic reactions: dielectric, electrostatic and steric stabilization of the carbonium ion in the reaction of lysozyme, J. Mol. Biol. 103 (1976) 227–249.
[18] D.B. Kitchen, H. Decornez, J.R. Furr, J. Bajorath, Docking and scoring in virtual screening for drug discovery: methods and applications, Nat. Rev. Drug Discov. 3 (2004) 935–949.
[19] C. McInnes, Virtual screening strategies in drug discovery, Curr. Opin. Chem. Biol. 11 (2007) 494–502.
[20] P. Badrinarayan, G. Narahari Sastry, Virtual high throughput screening in new lead identification, Comb. Chem. High Throughput Screen. 14 (2011) 840–860.
[21] D.A. Evans, S. Neidle, Virtual screening of DNA minor groove binders, J. Med. Chem. 49 (2006) 4232–4238.
[22] A.M. Sobhani, S.R. Amini, J.D. Tyndall, E. Azizi, M. Daneshtalab, A. Khalaj, A theory of mode of action of azolylalkylquinolines as DNA binding agents using automated flexible ligand docking, J. Mol. Graph. Model. 25 (2006) 459–469.
[23] H.K. Srivastava, M. Chourasia, D. Kumar, G.N. Sastry, Comparison of computational methods to model DNA minor groove binders, J. Chem. Inf. Model. 51 (2011) 558–571.
[24] E.B. Kelly, J.A. Tuszynski, M. Klobukowski, QM and QM/MD simulations of the Vinca alkaloids docked to tubulin, J. Mol. Graph. Model. 30 (2011) 54–66.
[25] O. Trott, A.J. Olson, AutoDock Vina: improving the speed and accuracy of docking with a new scoring function, efficient optimization, and multithreading, J. Comput. Chem. 31 (2010) 455–461.
[26] A. Gupta, A. Gandhimathi, P. Sharma, B. Jayaram, ParDOCK: an all atom energy based Monte Carlo docking protocol for protein–ligand complexes, Protein Pept. Lett. 14 (2007) 632–646.
[27] D. Seeliger, B.L. de Groot, Ligand docking and binding site analysis with PyMOL and Autodock/Vina, J. Comput. Aided Mol. Des. 24 (2010) 417–422.
[28] M.W. Chang, C. Ayeni, S. Breuer, B.E. Torbett, Virtual screening for HIV protease inhibitors: a comparison of AutoDock 4 and Vina, PLoS ONE 5 (2010) e11955.
[29] Y. Takatsuka, C. Chen, H. Nikaido, Mechanism of recognition of compounds of diverse structures by the multidrug efflux pump AcrB of *Escherichia coli*, Proc. Natl. Acad. Sci. U.S.A. 107 (2010) 6559–6565.
[30] M.M. Islam, M. Chakraborty, P. Pandya, A. Al Masum, N. Gupta, S. Mukhopadhyay, Binding of DNA with Rhodamine B: spectroscopic and molecular modeling studies, Dyes Pigment. 99 (2013) 412–422.
[31] D.R. Houston, M.D. Walkinshaw, Consensus docking: improving the reliability of docking in a virtual screening context, J. Chem. Inf. Model. 53 (2013) 384–390.
[32] R.M. Bieganski, M.L. Yarmush, Novel ligands that target the mitochondrial membrane protein mitoNEET, J. Mol. Graph. Model. 29 (2011) 965–973.
[33] T. Vreven, K. Morokuma, O. Farkas, H.B. Schlegel, M.J. Frisch, Geometry optimization with QM/MM, ONIOM, and other combined methods. I. Microiterations and constraints, J. Comput. Chem. 24 (2003) 760–769.
[34] M.J. Frisch, G.W. Trucks, H.B. Schlegel, G.E. Scuseria, M.A. Robb, J.R. Cheeseman, G. Scalmani, V. Barone, B. Mennucci, G.A. Petersson, H. Nakatsuji, M. Caricato,

X. Li, H.P. Hratchian, A.F. Izmaylov, J. Bloino, G. Zheng, J.L. Sonnenberg, M. Hada, M. Ehara, K. Toyota, R. Fukuda, J. Hasegawa, M. Ishida, T. Nakajima, Y. Honda, O. Kitao, H. Nakai, T. Vreven, J.A. Montgomery Jr., J.E. Peralta, F. Ogliaro, M. Bearpark, J.J. Heyd, E. Brothers, K.N. Kudin, V.N. Staroverov, R. Kobayashi, J. Normand, K. Raghavachari, A. Rendell, J.C. Burant, S.S. Iyengar, J. Tomasi, M. Cossi, N. Rega, N.J. Millam, M. Klene, J.E. Knox, J.B. Cross, V. Bakken, C. Adamo, J. Jaramillo, R. Gomperts, R.E. Stratmann, O. Yazyev, A.J. Austin, R. Cammi, C. Pomelli, J.W. Ochterski, R.L. Martin, K. Morokuma, V.G. Zakrzewski, G.A. Voth, P. Salvador, J.J. Dannenberg, S. Dapprich, A.D. Daniels, Ö. Farkas, J.B. Foresman, J.V. Ortiz, J. Cioslowski, D.J. Fox, Gaussian 09, Gaussian, Inc., Wallingford CT, 2009.

[35] D. Mishra, S. Pal, S. Krishnamurty, Understanding the molecular conformations of Na-dimyristoylphosphatidylglycerol (DMPG) using DFT-based method, Mol. Simulat. 37 (2011) 953–963.

[36] M.L. Vueba, M.E. Pina, F. Veiga, J.J. Sousa, L.A. de Carvalho, Conformational study of ketoprofen by combined DFT calculations and Raman spectroscopy, Int. J. Pharm. 307 (2006) 56–65.

[37] C.A. Lipinski, F. Lombardo, B.W. Dominy, P.J. Feeney, Experimental and computational approaches to estimate solubility and permeability in drug discovery and development settings, Adv. Drug Deliver. Rev. 23 (1997) 3–25.

[38] C. Lipinski, A. Hopkins, Navigating chemical space for biology and medicine, Nature 432 (2004) 855–861.

[39] E. Nogales, Structural insights into microtubule function, Annu. Rev. Biochem. 69 (2000) 277–302.

[40] Z. Moravek, S. Neidle, B. Schneider, Protein and drug interactions in the minor groove of DNA, Nucleic Acids Res. 30 (2002) 1182–1191.

[41] S. Neidle, DNA minor-groove recognition by small molecules (up to 2000), Nat. Prod. Rep. 18 (2001) 291–309.

[42] A. Varshney, P. Sen, E. Ahmad, M. Rehan, N. Subbarao, R.H. Khan, Ligand binding strategies of human serum albumin: how can the cargo be utilized, Chirality 22 (2010) 77–87.

[43] M. Fasano, S. Curry, E. Terreno, M. Galliano, G. Fanali, P. Narciso, S. Notari, P. Ascenzi, The extraordinary ligand binding properties of human serum albumin, IUBMB Life 57 (2005) 787–796.

[44] P. Ascenzi, A. Bocedi, S. Notari, G. Fanali, R. Fesce, M. Fasano, Allosteric modulation of drug binding to human serum albumin, Mini Rev. Med. Chem. 6 (2006) 483–489.

[45] P. Ascenzi, M. Fasano, Allostery in a monomeric protein: the case of human serum albumin, Biophys. Chem. 148 (2010) 16–22.

[46] A. Ahmed-Ouameur, S. Diamantoglou, M.R. Sedaghat-Herati, S. Nafisi, R. Carpentier, H.A. Tajmir-Riahi, The effects of drug complexation on the stability and conformation of human serum albumin: protein unfolding, Cell Biochem. Biophys. 45 (2006) 203–213.

[47] R.L. Gundry, Q. Fu, C.A. Jelinek, J.E. Van Eyk, R.J. Cotter, Investigation of an albumin-enriched fraction of human serum and its albuminome, Proteom. Clin. Appl. 1 (2007) 73–88.

[48] G. Fanali, A. di Masi, V. Trezza, M. Marino, M. Fasano, P. Ascenzi, Human serum albumin: from bench to bedside, Mol. Asp. Med. 33 (2012) 209–290.